

Heat capacities of $\text{PbBi}_{12}\text{O}_{19}(\text{s})$ and $\phi\text{-Pb}_5\text{Bi}_8\text{O}_{17}(\text{s})$

Rajesh Ganesan^a, R. Venkatakrisnan^a, R. Asuvathraman^a, K. Nagarajan^a,
T. Gnanasekaran^{a,*}, Raman S. Srinivasa^b

^a Chemistry Group, Indira Gandhi Centre for Atomic Research, Liquid Metals and Structural Chemistry Division, Kalpakkam 603102, Tamilnadu, India

^b Department of Metallurgical Engineering and Materials Science, Indian Institute of Technology Bombay, Mumbai 400076, India

Received 14 June 2005; received in revised form 9 September 2005; accepted 9 September 2005

Available online 10 October 2005

Abstract

Heat capacities of $\text{PbBi}_{12}\text{O}_{19}(\text{s})$ and $\phi\text{-Pb}_5\text{Bi}_8\text{O}_{17}(\text{s})$ were measured by differential scanning calorimetry in the temperature range 280–820 K and 280–660 K, respectively. $\text{PbBi}_{12}\text{O}_{19}(\text{s})$ and $\phi\text{-Pb}_5\text{Bi}_8\text{O}_{17}(\text{s})$ showed order–disorder transitions whose onset temperatures are 520 K and 700 K, respectively. The measured heat capacities of $\text{PbBi}_{12}\text{O}_{19}(\text{s})$ and $\phi\text{-Pb}_5\text{Bi}_8\text{O}_{17}(\text{s})$ as a function of temperature are expressed as:

$$C_p < \text{PbBi}_{12}\text{O}_{19} > (\text{JK}^{-1} \text{mol}^{-1}) = 791.68 + 112.18 \times 10^{-3} T - 13.58 \times 10^6 T^{-2} \quad (280 - 820 \text{ K})$$

$$C_p < \phi\text{-Pb}_5\text{Bi}_8\text{O}_{17} > (\text{JK}^{-1} \text{mol}^{-1}) = 700.02 + 161.58 \times 10^{-3} T - 12.85 \times 10^6 T^{-2} \quad (280 - 660 \text{ K})$$

Enthalpy increments, entropies and Gibbs energy functions were derived from the measured heat capacity data.

© 2005 Elsevier B.V. All rights reserved.

Keywords: Pb–Bi–O; Heat capacity; High temperature X-ray diffraction; Electrical conductivity; Order–disorder transition

1. Introduction

Liquid lead and lead–bismuth eutectic (LBE) alloy are currently being explored for service as spallation target and coolant in accelerator driven systems (ADS) [1,2]. Though these coolants are corrosive to structural steels, corrosion can be minimized by forming a protective oxide layer by control of oxygen concentration in the coolant [3]. Effective oxygen control requires understanding of the thermodynamics of the Pb–Bi–O system. The pseudo binary phase diagram of PbO–Bi₂O₃ system has been established and four ternary compounds are known, viz., $\text{PbBi}_{12}\text{O}_{19}(\text{s})$, $\text{Pb}_2\text{Bi}_6\text{O}_{11}(\text{s})$, $\text{Pb}_5\text{Bi}_8\text{O}_{17}(\text{s})$ and $\text{Pb}_3\text{Bi}_2\text{O}_6(\text{s})$ [4]. $\text{Pb}_2\text{Bi}_6\text{O}_{11}(\text{s})$ and $\text{Pb}_3\text{Bi}_2\text{O}_6(\text{s})$ are stable only in narrow temperature ranges viz., 848–882 K and 853–876 K, respectively. The compounds $\text{PbBi}_{12}\text{O}_{19}(\text{s})$ and $\text{Pb}_5\text{Bi}_8\text{O}_{17}(\text{s})$ are stable from room temperature up to ~988 K and ~868 K, respectively. $\text{PbBi}_{12}\text{O}_{19}(\text{s})$ exists in cubic form (bcc) [5–7]. $\text{Pb}_5\text{Bi}_8\text{O}_{17}(\text{s})$ has at least three polymorphs of which $\beta_2\text{-Pb}_5\text{Bi}_8\text{O}_{17}(\text{s})$ and $\phi\text{-Pb}_5\text{Bi}_8\text{O}_{17}(\text{s})$ are low temperature phases

[8–10]. $\beta_2\text{-Pb}_5\text{Bi}_8\text{O}_{17}(\text{s})$ is a high temperature phase [8–10], which exhibits high oxygen ion conductivity [11] thus making it suitable for use as an oxygen selective membrane [12]. $\beta_2\text{-Pb}_5\text{Bi}_8\text{O}_{17}(\text{s})$, a meta stable phase with tetragonal structure, is formed when quenched from 883 K either in air or nitrogen while ϕ -phase is formed on slow cooling [10,13]. The structure of $\phi\text{-Pb}_5\text{Bi}_8\text{O}_{17}(\text{s})$ has been reported to be triclinic [8,9,14–16]. Although data on structural characteristics of these compounds have been reported, their thermodynamic properties have not yet been investigated.

In the present work, heat capacities of $\text{PbBi}_{12}\text{O}_{19}(\text{s})$ and $\phi\text{-Pb}_5\text{Bi}_8\text{O}_{17}(\text{s})$ have been measured as a function of temperature by differential scanning calorimetry. Enthalpy increments, entropies and Gibbs energy functions of these compounds have been derived from the heat capacity data.

2. Experimental

2.1. Sample preparation

Ternary compounds $\text{PbBi}_{12}\text{O}_{19}(\text{s})$ and $\phi\text{-Pb}_5\text{Bi}_8\text{O}_{17}(\text{s})$ were prepared by solid-state reaction between high purity PbO

* Corresponding author. Tel.: +91 4114 280302; fax: +91 4114 280065.
E-mail address: gmani@igcar.ernet.in (T. Gnanasekaran).

Table 1
Thermodynamic functions of $\text{PbBi}_{12}\text{O}_{19}(\text{s})$

Temperature (K)	C_p ($\text{J K}^{-1} \text{mol}^{-1}$)		$(H_T^0 - H_{298}^0)$ (J mol^{-1})	S_T^0 ($\text{J K}^{-1} \text{mol}^{-1}$)	$-(G_T^0 - H_{298}^0)/T$ ($\text{J K}^{-1} \text{mol}^{-1}$)
	Measured	Fit			
280	649	650	–	–	–
298.15	–	672	0	901	901
300	677	674	1246	905	901
400	753	752	73023	1111	929
500	791	793	150450	1284	983
600	819	821	231261	1431	1046
700	836	842	314487	1559	1110
800	861	860	399644	1673	1173

(99.999 mass%, M/s. Aldrich, USA) and Bi_2O_3 (99.99 mass%, M/s. Nuclear Fuel Complex, India) powders taken in stoichiometric mole ratios. The oxide powders were mixed thoroughly, ground with a mortar and pestle and compacted into discs. The discs in an alumina crucible were placed inside a quartz tube which was evacuated and filled with argon gas two to three times and sealed under vacuum. $\text{PbBi}_{12}\text{O}_{19}(\text{s})$ was prepared by heating the compacted oxide mixture at 908 K for 200 h while $\phi\text{-Pb}_5\text{Bi}_8\text{O}_{17}(\text{s})$ was prepared by heating at 823 K for 200 h with an additional intermediate step of grinding, mixing, pelletising and vacuum sealing. The compounds were cooled slowly ($\sim 5 \text{ K min}^{-1}$) after the heat treatment. The products obtained were characterised by X-ray diffraction. The XRD patterns of $\text{PbBi}_{12}\text{O}_{19}(\text{s})$ and $\text{Pb}_5\text{Bi}_8\text{O}_{17}(\text{s})$ matched the patterns reported in JCPDS file 24–1184 for the cubic phase and 52–1497 for the triclinic phase [17].

2.2. Calorimetric measurements

A heat flux differential scanning calorimeter, model number DSC821e/700 of M/s. Mettler Toledo GmbH, Switzerland was used in this study. The samples for DSC measurements were pelletised and hermetically sealed in 40 μl Al-pans. High purity argon gas at a flow rate of 50 ml min^{-1} was used as the purge gas. DSC measurements were done from 280 K to 820 K at a heating rate of 10 K min^{-1} . Additionally, measurements with heating rates of 5 K min^{-1} and 20 K min^{-1} were also carried out. A disc of sapphire was used as the standard for heat rate calibration. The heat capacity data of sapphire given by National Institute of Standards and Technology (NIST), USA was used for computing the heat capacities of the samples [18]. A three-segment temperature program was used. The first segment lasting for 5 min was isothermal at the initial temperature, the second was with a heating rate of 10 K min^{-1} and the third, lasting for 5 min was again isothermal at the final temperature. The samples were characterized by XRD before and after the calorimetric runs. The data at each temperature is derived as the mean of 10 measurements and the associated relative standard deviations is <3%.

2.3. High temperature X-ray diffraction studies

High temperature X-ray diffraction studies were done with a Philips-X'pert[®] system with Cu $K\alpha$ radiation. The sample was

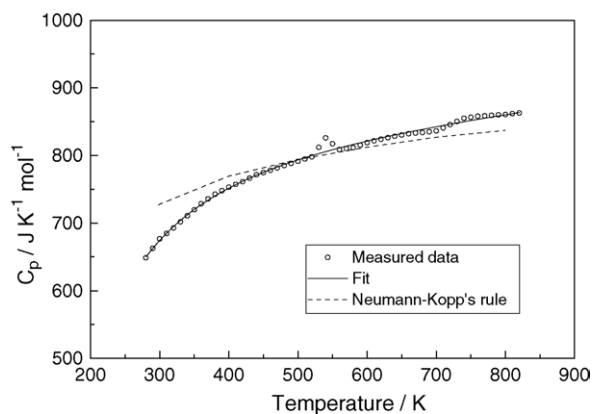
loaded as a thin layer over a thin, resistance-heated, platinum foil in the high temperature attachment of the X-ray diffractometer. Temperature was controlled within $\pm 1 \text{ K}$. A heating rate of 30 K min^{-1} and a holding time of 10 min at each temperature of measurement were adopted. Data was recorded under a vacuum of $\sim 10^{-5}$ Torr as well as in static air.

2.4. Electrical conductivity measurements

Pellets of $\text{PbBi}_{12}\text{O}_{19}(\text{s})$ and $\text{Pb}_5\text{Bi}_8\text{O}_{17}(\text{s})$ (10 mm diameter and 2–3 mm thickness) were prepared by compacting the powders under 20 MPa pressure and sintering at 923 K and 823 K, respectively, for 20 h under argon. A sample pellet was mounted between two spring-loaded platinum foils of identical dimensions and placed inside a quartz chamber, which in turn was heated by a furnace. The conductivity of the pellet was measured under flowing argon ($\sim 30 \text{ ml min}^{-1}$) with a frequency response analyser (model SI 1255 of Solartron, M/s. Schlumberger, UK) coupled to an electrochemical interface (model 1286 of Solartron, M/s. Schlumberger, UK) in the frequency range of 1 Hz–1 MHz. The data were analysed by a deconvolution technique using Boukamp analysis program [19]. The conductivity values were reproducible during heating, cooling and random cycles. The samples were characterized by XRD before and after the electrical conductivity measurements.

3. Results and discussion

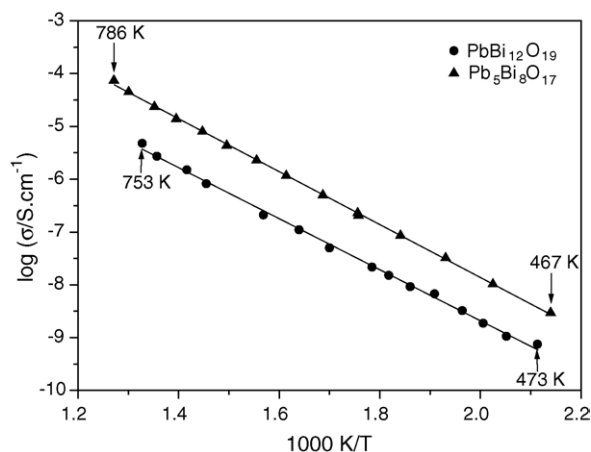
The heat capacity of $\text{PbBi}_{12}\text{O}_{19}(\text{s})$ is shown in Table 1 and Fig. 1. It can be seen from Fig. 1 that there is a small but distinct peak at 540 K with an onset temperature of 520 K in the heat capacity data, indicating the presence of a phase transition. To confirm the existence and to delineate the nature of the phase transition, high temperature X-ray diffraction studies were carried out at 480 K, 540 K, 600 K and 773 K. The XRD pattern does not exhibit any change with increase in temperature. Since the atomic scattering factors for lead and bismuth are very close, an order–disorder type transition is not expected to change the XRD pattern [20] except for a small shift due to lattice expansion. Murray et al. [5] has also indicated that it is difficult to obtain definite information about the distribution of Pb^{2+} over the lattice sites because of similar

Fig. 1. Heat capacity data of PbBi₁₂O₁₉(s).

scattering lengths of Pb²⁺ and Bi³⁺. Hence, it is concluded that the transition is an order–disorder one. Results of the additional DSC measurements at heating rates of 5 K min⁻¹ and 20 K min⁻¹ have shown that the onset temperatures were within ±1 K and the variation of the peak area was ±10%. These results indicate that the transition observed is fast and hence the heat capacity of the compound is independent of the scan rate.

Electrical conductivity measurements were carried out in the range 473–753 K to unravel the nature of phase transition. Since the scatter in the impedance data was higher at lower temperatures due to the high resistivity of the sample, the conductivity measurements were not done below 473 K. Fig. 2 shows the electrical conductivity of PbBi₁₂O₁₉(s) in argon as a function of temperature. The observed variation of conductivity with temperature can be represented as $\log \sigma = A - E/kT$, where A is the Arrhenius constant, E the activation energy for the conduction process, k the Boltzmann constant and T is the Kelvin temperature. The activation energy was calculated to be 0.42 ± 0.02 eV. Although the number of data points below 540 K are limited, there is no significant change in the temperature dependence of electrical conductivity indicating that the order–disorder transition in PbBi₁₂O₁₉(s) does not involve any significant change in electrical conductivity.

Since the order–disorder transition does not affect the C_p values except in the temperature range of 520–560 K, heat capacity values of PbBi₁₂O₁₉(s) measured at other tempera-

Fig. 2. Arrhenius plot for electrical conductivity of PbBi₁₂O₁₉(s) and ϕ -Pb₅Bi₈O₁₇(s) in argon atmosphere.

tures were fitted to the following expression by the least squares method:

$$C_p(\text{PbBi}_{12}\text{O}_{19})(\text{J K}^{-1} \text{mol}^{-1}) = 791.68 + 112.18 \times 10^{-3}T - 13.58 \times 10^6 T^{-2}, \quad (280\text{--}820 \text{ K}) \quad (1)$$

The standard error of the fit is $\pm 4.21 \text{ J K}^{-1} \text{mol}^{-1}$. These fitted values are shown in Table 1 along with the measured values. These data on heat capacity of PbBi₁₂O₁₉(s) are the first to be reported.

The heat capacity of PbBi₁₂O₁₉(s) was computed by Neumann–Kopp's rule using heat capacity data for PbO(s) and Bi₂O₃(s) [21], and is compared with the measured values in Fig. 1. The experimental $C_{p,298\text{K}}$ is 7.5% lower than the estimated value. Assuming S_{298}^0 of PbBi₁₂O₁₉(s) to also be 7.5% lower than the value derived from Neumann–Kopp's rule, it was deduced to be $901 \text{ J K}^{-1} \text{mol}^{-1}$ from S_{298}^0 values of PbO(s) and Bi₂O₃(s), viz., $65.480 \text{ J K}^{-1} \text{mol}^{-1}$ and $151.461 \text{ J K}^{-1} \text{mol}^{-1}$, respectively [21]. To examine the validity of this assumption underlying this correction, the reported thermochemical data of ternary oxides in [21] were considered. The difference between the Gibbs free energies of formation per oxygen atom of PbO and Bi₂O₃ at 298.15 K is ~ 25 kJ. Ternary oxide systems were chosen such that the difference between the Gibbs free energies of formation per oxygen atom of the constituent binary oxides is less than or equal to ~ 35 kJ. The differences between

Table 2
Thermodynamic functions of ϕ -Pb₅Bi₈O₁₇(s)

Temperature (K)	C_p (J K ⁻¹ mol ⁻¹)		$(H_T^0 - H_{298}^0)$ (J mol ⁻¹)	S_T^0 (J K ⁻¹ mol ⁻¹)	$-(G_T^0 - H_{298}^0)/T$ (J K ⁻¹ mol ⁻¹)
	Measured	Fit			
280	582	581	–	–	–
298.15	–	604	0	826	826
300	606	606	1119	830	826
400	685	684	66068	1016	851
500	726	729	136916	1174	900
600	760	761	211521	1310	957
700	771	–	–	–	–
800	861	–	–	–	–

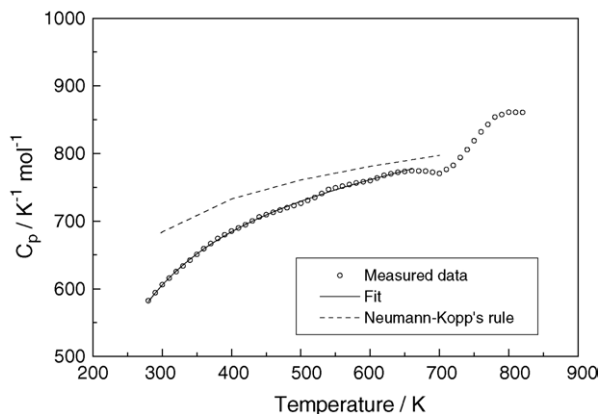


Fig. 3. Heat capacity data of ϕ -Pb₅Bi₈O₁₇(s).

the reported heat capacity values [21] and those estimated using Neumann–Kopp’s rule ($\Delta C_{p,298K}$) for these ternary oxides were calculated. The corresponding values for ΔS_{298K}^0 were also computed from the entropy data listed in [21]. For $\sim 67\%$ of these systems, $\Delta C_{p,298K}$ and ΔS_{298K}^0 have the same sign though the magnitudes differ. Hence, the above correction procedure for estimating S_{298}^0 was adopted in this work. Similar approach has been adopted for the estimation of the S_{298}^0 of BaThO₃ described elsewhere [22]. Using the value for S_{298}^0 thus estimated and expression (1) for heat capacity, the enthalpy increments, entropies and Gibbs energy functions of PbBi₁₂O₁₉(s) were computed as shown in Table 1.

The experimental heat capacity of ϕ -Pb₅Bi₈O₁₇(s) as a function of temperature is shown in Table 2 and Fig. 3. Fig. 3 shows an abnormal increase of C_p with increase in temperature from 700 K and attained the normal pattern only above 800 K. This observation indicates that ϕ -Pb₅Bi₈O₁₇(s) undergoes a second order transition whose onset temperature is 700 K.

High temperature X-ray diffraction studies and electrical conductivity measurements were also carried out for this compound to characterise the phase transition. XRD patterns obtained at 623 K, 673 K, 723 K, 773 K and 823 K showed no phase transition. We propose that an order–disorder type transition also takes place with this compound at 700 K. Fig. 2 shows the electrical conductivity of ϕ -Pb₅Bi₈O₁₇(s) in argon as a function of temperature. The observed variation of conductivity with temperature in the temperature range of measurement (467–786 K) can be represented as $\log \sigma = A - E/kT$. The activation energy was calculated to be 0.43 ± 0.01 eV. The electrical conductivity also does not vary significantly during the order–disorder transition.

Because of the large monotonous increase in C_p between 700 K and 800 K, preceded by a small dip in the temperature range of 660–700 K, the measured heat capacity values of ϕ -Pb₅Bi₈O₁₇(s) from 280 K to 660 K were fitted to the following expression by using the least squares method.

$$C_p(\text{J K}^{-1} \text{mol}^{-1}) = 700.02 + 161.58 \times 10^{-3}T - 12.85 \times 10^6 T^{-2}, \quad (280\text{--}660 \text{ K}) \quad (2)$$

The standard error of the fit is $\pm 1.60 \text{ J K}^{-1} \text{mol}^{-1}$. The heat capacity values computed from Eq. (2) are shown in Table 2 along with measured values. S_{298}^0 values of ϕ -Pb₅Bi₈O₁₇(s) were also estimated as in the case of PbBi₁₂O₁₉(s). The experimental $C_{p,298}$ is 11.5% lower than the value estimated by invoking Neumann–Kopp’s rule. Assuming that the S_{298}^0 value of ϕ -Pb₅Bi₈O₁₇(s) will also be 11.5% lower than the value computed using Neumann–Kopp’s rule, the S_{298}^0 value of ϕ -Pb₅Bi₈O₁₇(s) was computed to be $826 \text{ J K}^{-1} \text{mol}^{-1}$. Using this value and expression (2) for heat capacity, the enthalpy increments, entropies and Gibbs energy functions of the compound in the temperature range of 280–660 K were computed and are shown in Table 2. For ϕ -Pb₅Bi₈O₁₇(s) also, the present C_p data are the first to be reported.

Acknowledgements

The authors acknowledge Ms. P.C. Clinsha, Mahatma Gandhi University, Kottayam for her help during DSC measurements and Mr. Santosh Bobade, Department of Metallurgical Engineering and Materials Science, IIT Bombay for his help in recording high temperature X-ray diffraction data. The authors also acknowledge Dr. K.V.G. Kutty for helpful discussions.

References

- [1] B.F. Gromov, (Ed.), Heavy Liquid Metal Coolants in Nuclear Technology (HLMC-98), vols. 1 and 2, SSC RF-IPPE, Obninsk, 1999.
- [2] J. Zhang, N. Li, Review of studies of fundamental issues in LBE corrosion, Los Alamos National Laboratory, LA-UR-04-0869, 2004.
- [3] N. Li, *J. Nucl. Mater.* 300 (2002) 73–81.
- [4] R.M. Biefeld, S.S. White, *J. Am. Ceram. Soc.* 64 (1981) 182–184.
- [5] A.D. Murray, C.R.A. Catlow, F. Beech, J. Drennan, *J. Solid State Chem.* 62 (1986) 290–296.
- [6] S. Mazumdar, *Ind. J. Phys.* 67A (1993) 45–52.
- [7] N. Rangavittal, T.N. Gururow, C.N.R. Rao, *Eur. J. Solid State Inorg. Chem.* 31 (1994) 409–422.
- [8] Y. Zhang, N. Sammes, Y. Du, *Solid State Ionics* 124 (1999) 179–184.
- [9] M. Gemmi, L. Righi, G. Calestani, A. Migliori, A. Speghini, M. Santarosa, M. Bettinelli, *Ultramicroscopy* 84 (2000) 133–142.
- [10] M.G. Fee, N.M. Sammes, G. Tompsett, T. Stoto, A.M. Cartner, *Solid State Ionics* 95 (1997) 183–189.
- [11] F. Honnart, J.C. Boivin, D. Thomas, K.J. De Vries, *Solid State Ionics* 9/10 (1983) 921–924.
- [12] M.G. Fee, N.J. Long, *Solid State Ionics* 86–88 (1996) 733–737.
- [13] N.M. Sammes, R.J. Phillips, M.G. Fee, *Solid State Ionics* 69 (1994) 121–126.
- [14] A. Watanabe, Y. Kitami, S. Takenouchi, J.O. Bovin, N. Sammes, *J. Solid State Chem.* 144 (1999) 195–204.
- [15] M. Santarosa, L. Righi, M. Gemmi, A. Speghini, A. Migliori, G. Calestani, M. Bettinelli, *J. Solid State Chem.* 144 (1999) 255–262.
- [16] L. Righi, G. Calestani, M. Gemmi, A. Migliori, M. Bettinelli, *Acta Cryst. B* 57 (2001) 237–243.
- [17] Powder diffraction files, Joint Committee on Powder Diffraction Data (JCPDS), International Centre for Diffraction Data, PCPDFWIN Version: 2.02, 1999 (ICDD card number: 24-1184 for PbBi₁₂O₁₉ and 52-1497 for ϕ -Pb₅Bi₈O₁₇).

- [18] Synthetic Sapphire α -Al₂O₃, Certificate of Standard Reference Materials 720, National Bureau of Standards, US Department of Commerce, Washington, USA, 1982.
- [19] B.A. Boukamp, *Solid State Ionics* 20 (1986) 31–44.
- [20] B.D. Cullity, *Elements of X-ray Diffraction*, Addison-Wesley Publishing Company Inc., Massachusetts, 1956, p. 474.
- [21] O. Knacke, O. Kubaschewski, K. Hesselmann (Eds.), *Thermochemical Properties of Inorganic Substances*, vol. 2, Springer, Berlin, 1991.
- [22] R. Venkatakrishnan, K. Nagarajan, P.R. Vasudeva Rao, *J. Nucl. Mater.* 299 (2001) 28–31.